Vol. 49 — N° 4 12 25 p. 839 – 855

GEOSTANDARDS and GEOANALYTICAL RESEARCH

Determination of Sm, Nd Mass Fractions and $^{143}Nd/^{144}Nd$ Ratios in Mafic-Ultramafic Rock Reference Materials by MC-ICP-MS

Qindi **Wei** (1, 2), Yueheng **Yang** (1, 2)*, Zhuyin **Chu** (1, 2), Shitou **Wu** (1, 2), Hao **Wang** (1), Chao **Huang** (1, 2), Lei **Xu** (1, 2), Liewen **Xie** (1, 2), Jinhui **Yang** (1) and Fuyuan **Wu** (1)

(1) State Key Laboratory of Lithospheric and Environmental Coevolution, Institute of Geology and Geophysics, Chinese Academy of Sciences, Beijing 100029, P.R. China
(2) Institutional Centre for Shared Technologies and Facilities, Institute of Geology and Geophysics, Chinese Academy of Sciences, Beijing 100029, P.R. China
* Corresponding author. e-mail: yangyueheng@mail.iggcas.ac.cn

In this work, we describe a measurement procedure that provides high precision measurement results of samarium (Sm) and neodymium (Nd) mass fractions, as well as $^{143}Nd/^{144}Nd$ ratios in mafic–ultramafic rock reference materials, using isotope dilution (ID) multi-collector inductively coupled plasma-mass spectrometry (MC-ICP-MS). This technique is superior in terms of intermediate measurement precision, simplicity and rapidity compared with thermal ionisation mass spectrometry (TIMS) based on high-sensitivity NdO^+ techniques. Samples were spiked with a ^{149}Sm-^{150}Nd enriched tracer and then digested using a commonly used protocol involving HF, HNO_3 and $HClO_4$. The sample solution was directly purified using a single DGA resin column to obtain Sm and Nd fractions with high purity and recovery. The samples including five serpentinised dunites (DZE-1, DZE-2, NIM-D, JP-1, DTS-2b), a harzburgite (HARZ01), a serpentinised harzburgite (MUH-1; certified reference material according to ISO Guides for major and trace elements), two serpentinised lherzolites (WPR-1a, UB-N), a komatiite (OKUM; certified reference material according to ISO Guides), a pyroxenite (NIM-P) and a norite (NIM-N), which encompass various rock types with very low Sm and Nd mass fractions (from ng g^{-1} to sub-ng g^{-1} levels), were analysed. The measurement results of these reference materials (RMs), demonstrate that the measured $^{147}Sm/^{144}Nd$ and $^{143}Nd/^{144}Nd$ ratios are in good agreement with previously published values obtained by the TIMS and MC-ICP-MS techniques. Notably for OKUM, HARZ01, DZE-1, DZE-2 and NIM-D, this study provides the first reported data on $^{143}Nd/^{144}Nd$ ratios. This protocol has great potential for Sm–Nd analysis of ultra-low Nd abundance samples in geochemistry, cosmochemistry and environmental sciences (e.g., peridotite, garnet, meteorites, dust, etc.). Therefore, the high sample throughput inherent to MC-ICP-MS can be fully exploited in these research fields.

Keywords: mafic-ultramafic rock, ultra-low Nd abundance geological materials, Sm–Nd isotopes, MC-ICP-MS, DGA resin.

Received 22 Nov 24 – Accepted 25 Jun 25

As a powerful geochemical tracer and chronometer, the classical ^{147}Sm-^{143}Nd isotopic system has been extensively used in geochemistry and cosmochemistry (Faure and Mensing 2004). Due to the long half-life of ^{147}Sm (106 billion years), the radiogenic variation of the $^{143}Nd/^{144}Nd$ isotope ratio is comparatively small in most geological samples. Therefore, since the 1960s, the classical multi-collector thermal ionisation mass spectrometry (TIMS) technique has been regarded as the benchmark for Nd isotopic measurements because of its inherently high precision (Lugmair and Marti 1978, Lugmair and Galer 1992, Li *et al.* 2007, Chu *et al.* 2009, Harvey and Baxter 2009). Recently, multi-collector inductively coupled plasma-mass spectrometry (MC-ICP-MS) has become a routine and competitive technique for $^{143}Nd/^{144}Nd$ isotope measurements, offering relatively simplified chemical purification and high sample throughput with precision comparable to classical TIMS. Moreover, it is

doi: 10.1111/ggr.70006

now possible to directly analyse $^{143}Nd/^{144}Nd$ ratios of relatively Nd-enriched minerals (e.g., allanite, apatite, titanite, monazite, perovskite, etc.) with high spatial resolution on a sub-grain scale using MC-ICP-MS coupled with a laser ablation (LA) system (Yang *et al.* 2009, 2014, 2019, 2022, Ma *et al.* 2019). In summary, MC-ICP-MS has become the technique of choice for routine analysis of Sm and Nd mass fraction and $^{143}Nd/^{144}Nd$ ratio at sub-microgram levels in geological samples (Nd > 1 µg g^{-1}).

As an important tracer of geological petrogenesis, measuring the isotopic signatures of $^{147}Sm/^{144}Nd$ and $^{143}Nd/^{144}Nd$ in ultra-low Nd abundance geological materials (Nd < 0.5 µg g^{-1}) has become increasingly significant. These materials include single grains of garnet, as well as separated minerals from meteorites and ultramafic rocks such as lherzolite, harzburgite and dunite. Precise measurements of these isotopic ratios are essential for obtaining highly accurate Sm–Nd ages and providing relevant geochemical constraints (Griselin *et al.* 2001, Shibata and Yoshikawa 2004, Li *et al.* 2007, Chu *et al.* 2009, Harvey and Baxter 2009, Huang *et al.* 2012, Xiong *et al.* 2016). Nevertheless, measurements with suitable uncertainty for Sm and Nd mass fractions, as well as $^{143}Nd/^{144}Nd$ ratios in ultra-low Nd abundance geological materials, are challenging. This challenge arises from the strong partition, coprecipitation and surface adsorption of these sample in fluorides, primarily MgF_2, formed during the HF-assisted digestion of high MgO ($w > 35\%$) ultramafic rocks. This leads to low recovery yields for these elements (Shibata and Yoshikawa 2004, Qi *et al.* 2005, Sun *et al.* 2013). Because Nd can be ionised more efficiently as NdO^+ than as Nd^+ on TIMS, classical TIMS- NdO^+ technique is still regarded as the most powerful measurement principle for isotope ratio measurements of small amounts of Nd. However, this method is tedious and time-consuming, as it necessitates strict purification steps. Nd must be separated not only from Sm but also from cerium (Ce) and praseodymium (Pr) due to isobaric interference from CeO^+ and PrO^+ on NdO^+. Additionally, this technique requires extensive filament preparation and complex, hours-long mass spectrometric measurements (e.g., oxygen correction) (Griselin *et al.* 2001, Harvey and Baxter 2009, Chu *et al.* 2014a). Given these challenges, few publications present Sm–Nd isotopic data for ultra-low Nd abundance geological samples, even though this system has the potential to elucidate important geochemical processes (Griselin *et al.* 2001, Shibata and Yoshikawa 2004, Li *et al.* 2007, Chu *et al.* 2009, Harvey and Baxter 2009, Xiong *et al.* 2016). For the same reasons, there is limited Nd isotopic data for mafic-ultramafic rock reference materials (RMs) containing less than 0.5 µg g^{-1} Nd (Li *et al.* 2007, Chu *et al.* 2009, Harvey and Baxter 2009), except for $^{143}Nd/^{144}Nd$ ratios of PCC-1, JP-1 and DTS-2 determined by ID-TIMS based on the NdO^+ technique (Shibata and Yoshikawa 2004, Chu *et al.* 2009). Notably, PCC-1 is no longer commercially available, and JP-1 is nearing stock depletion, which are therefore not recommended for use as reference materials in modern geochemical studies. In summary, this scarcity of data is certainly due to the difficulty of Sm–Nd isotopic analyses of ultramafic rocks.

In recent years, scientific investigations have strategically addressed analytical limitations through optimisation of instrumental configurations and refinement of chromatographic separation protocols. Lately, a study employed MC-ICP-MS combined with a membrane desolvating system and highly sensitive cones (jet sample cone and X skimmer cone) to measure the Nd isotope ratios of serpentinite UB-N (~ 0.5 µg g^{-1} Nd), utilising a three-step ion exchange chromatography to isolate Nd from the samples (Zhou *et al.* 2024). These conventional isotope dilution methodologies typically necessitate laborious two- or three-stage chemical purification procedures followed by TIMS or MC-ICP-MS to determine Sm-Nd isotopic ratios, involving: (1) rare earth element (REE) isolation from sample matrices via cation-exchange chromatography (AG50W-X8/X12 resins) post-digestion, followed by (2) complete Sm-Nd separation using extraction chromatographic resins (e.g., P204, P507, Ln) (Chu *et al.* 2009, Yang *et al.* 2011, Zhou *et al.* 2024). In studies over the past decade, a novel extraction material (DGA resin) containing the tetraoctyldiglycolamide extractant has been demonstrated to have significant potential for the removal of sample matrix components and the separation of Nd from Ce and Sm, indicating better applicability to the determination of Nd isotope ratios in geological samples (Pourmand *et al.* 2012, Retzmann *et al.* 2017, Wang *et al.* 2017). However, the separation efficiency of Sm and Nd in ultra-low Nd mass fraction geological materials with a single DGA resin column has not been systematically investigated.

The motivation of this work was to develop a rapid and simple analytical protocol for determining Sm and Nd mass fractions, as well as $^{143}Nd/^{144}Nd$ ratios, in ultra-low Nd abundance geological materials using MC-ICP-MS, while maintaining low measurement uncertainties. We established an improved chemical procedure utilising a single DGA resin column to obtain Sm and Nd fractions with high purity and recovery. Furthermore, we demonstrate the Sm and Nd mass fractions and $^{143}Nd/^{144}Nd$ ratios of RMs, which are identical to previously reported data obtained by the TIMS and MC-ICP-MS techniques at the 95% confidence level, thereby illustrating the robustness of our analytical protocol.

Additionally, we provide the first-ever report of $^{143}Nd/^{144}Nd$ ratios for OKUM, HARZ01, DZE-1, DZE-2 and NIM-D.

Experimental

All chemical purification and mass spectrometric measurements were performed at the State Key Laboratory of Lithospheric and Environmental Coevolution (SKLLEC), Institute of Geology and Geophysics (IGG), Chinese Academy of Sciences (CAS), Beijing. All chemical procedures were conducted in Class 100 fume hoods located within a suite of Class 1000 over-pressurised clean rooms. The measurement procedures for sample digestion, column chromatography and mass spectrometry are described in detail below.

Reagents and materials

High purity water (resistivity of 18.2 MΩ cm at 25 °C), produced by a Milli-Q system Millipore, was used for all sample chemical preparations. Concentrated hydrochloric, nitric and hydrofluoric acids (BV-III grade), sourced from the Beijing Institute of Chemical Reagents, were purified twice using a Savillex DST-1000 PFA sub-boiling distillation system (Minnetonka, MN, USA). $HClO_4$ (w = 70%) and high-purity H_3BO_3 from Acros Organics (Belgium) were used directly without further purification. A H_3BO_3 solution (w = 3%) in 3 mol l^{-1} HNO_3 was prepared as follows: 12 g of high-purity H_3BO_3 was weighed into a clean PFA beaker and dissolved in 300 ml of high purity water. Then, 100 ml of sub boiled 14 mol l^{-1} HNO_3 was added to the solution.

The CIT natural Sm–Nd mixture solution was obtained from the California Institute of Technology (Wasserburg *et al.* 1981). JNdi-1 solutions with mass fractions of 20 ng g^{-1}, 10 ng g^{-1}, 5 ng g^{-1} and 2 ng g^{-1} were used for measurement sessions (Tanaka *et al.* 2000). An Alfa Sm ICP calibration solution (Specpure, Stock No. 13854) from Alfa Aesar, Johnson Matthey Company, was used for mass bias correction of $^{147}Sm/^{149}Sm$ ratios. As an in-house isotope standard, a 5 ng g^{-1} Alfa Sm solution was prepared and used during the actual measurements. Cation exchange material, specifically DGA resin (2 ml volume, 100–150 µm particle size), was purchased from Eichrom Industries (Darien, IL, USA).

To evaluate and validate our measurement procedure, we utilised reference materials (RMs) of mafic and ultramafic rocks produced by various organisations and researchers: Serpentinised dunite DTS-2b from the United States Geological Survey (USGS); serpentinised lherzolite UB-N from the Service d'Analyse des Roches et des Minéraux, Centre de Recherches Pétrographiques et Géochimiques-Centre national de la recherche scientifique (SARM, CRPG-CNRS, France); serpentinised dunite JP-1 from the Geological Survey of Japan (GSJ); serpentinised lherzolite WPR-1a from the Canadian Certified Reference Materials Project (CCRMP, Canada); Komatiite OKUM and serpentinised harzburgite MUH-1 from the International Association of Geoanalysts (IAG). Harzburgite HARZ01 was provided by Thomas C. Meisel and detailed information from the Geo*PT* proficiency testing programme (round 38A) was used. Norite NIM-N, pyroxenite NIM-P and dunite NIM-D were used from the Council for Mineral Technology (MINTEK, South Africa), as well as the serpentinised dunites DZE-1 and DZE-2 from the National Research Centre for Certified Reference Materials (NRC-CRM, China).

Sample digestion

Approximately 50–500 mg of rock powder was weighed into a 7 ml or 15 ml round-bottom Savillex PFA screw-top capsule. Weighed aliquots of the mixed ^{149}Sm-^{150}Nd isotopically enriched tracer were added to the samples and then gently evaporated to dryness. The amounts of spike added were calculated based on the previously reported Sm and Nd mass fractions in these reference materials. The mixed ^{149}Sm-^{150}Nd spike solution was frequently calibrated using the CIT Sm–Nd calibration solution in our laboratory. Concentrated hydrofluoric acid (HF, 2 ml), nitric acid (HNO_3, 1 ml) and perchloric acid ($HClO_4$, 0.2 ml) were added to the samples. The capsules were capped and then heated on a hotplate at approximately 150 °C for one week. After cooling, the capsules were opened and the mass fractions were heated to evaporate $HClO_4$. Five millilitres of concentrated HNO_3 was added to the residue and then evaporated; this procedure was repeated. After cooling, the residue was dissolved in 5 ml of a H_3BO_3 solution (w = 3%) in 3 mol l^{-1} HNO_3. The capsules were again sealed and placed on a hot plate at approximately 100 °C overnight to dissolve the solid residues prior to chemical separation.

Column chemistry

The chemical isolation procedure using a single-step DGA column is shown in Table 1. First, the column was cleaned sequentially with 5 m l of 0.05 mol l^{-1} HCl, 10 ml of 3.5 mol l^{-1} HNO_3 + 0.2 mol l^{-1} HF and 5 ml of 7 mol l^{-1} HNO_3. After eluting all remaining elements, the column was

Table 1.
Sm and Nd chemical purification procedure using single DGA resin with Sr–Nd–Pb–Hf fraction (optional)

Step	Volume	Acid	Remark
Resin cleaning	5 ml (2.5 ml × 2)	0.05 mol l^{-1} HCl	Eluting remaining REE
Resin cleaning	10 ml (2.5 ml × 4)	3.5 mol l^{-1} HNO_3 + 0.2 mol l^{-1} HF	Eluting remaining Zr+Hf
Resin cleaning	5 ml (2.5 ml × 2)	7 mol l^{-1} HNO_3	Eluting remaining elements
Resin cleaning	5 ml (2.5 ml × 2)	Mill H_2O	Transfer
Preconditioning	10 ml (5 ml × 2)	3.5 mol l^{-1} HNO_3 + w = 3% H_3BO_3	
Loading sample	5 ml (5 ml × 1)	3.5 mol l^{-1} HNO_3 + w = 3% H_3BO_3	
Eluting matrix	10 ml (5 ml × 2)	3.5 mol l^{-1} HNO_3	5 ml Sr + Pb (optional)
Eluting matrix	24 ml (2 ml × 12)	12 mol l^{-1} HNO_3	Eluting major elements
Collecting Hf	20 ml (5 ml × 4)	3.5 mol l^{-1} HNO_3 + 0.2 mol l^{-1} HF	Hf (optional)
Eluting matrix	6 ml (2 ml × 3)	2 mol l^{-1} HCl	Eluting La, Ce, Pr
Collecting Nd	6 ml (2 ml × 3)	2 mol l^{-1} HCl	Nd
Collecting Sm	4 ml (2 ml × 2)	1 mol l^{-1} HCl	Sm

washed twice with high purity H_2O and then conditioned with 10 ml of 3.5 mol l^{-1} HNO_3 + w = 3% H_3BO_3. Next, the centrifuged sample solution was loaded onto the DGA columns in 5 ml of 3.5 mol l^{-1} HNO_3 + w = 3% H_3BO_3. After the sample solution had completely drained, 10 ml of 3.5 mol l^{-1} HNO_3 was added to remove matrix elements. At this stage, strontium (Sr) and lead (Pb) can optionally be collected in the first 5 ml of eluate. Residual major and transition elements, including calcium (Ca), were stripped using 24 ml of 12 mol l^{-1} HNO_3. Subsequently, hafnium (Hf) fractions (optional) were extracted from the column with 20 ml of 3.5 mol l^{-1} HNO_3 + 0.2 mol l^{-1} HF and gently evaporated to dryness. This fraction was taken up in 2 mol l^{-1} HF, diluted to 1.2 ml with 2% *v/v* HNO_3, and was then ready for Hf isotope ratio measurements. After this step, La, Ce and Pr were removed with a 6 ml wash of 2 mol l^{-1} HCl, followed by the elution of Nd with another 6 ml of 2 mol l^{-1} HCl. Finally, Sm was recovered with 4 ml of 1 mol l^{-1} HCl. The Nd and Sm fractions were collected in clean PFA beakers and evaporated to dryness, then taken up with 0.1 ml of 2 mol l^{-1} HCl and diluted to 1.2 ml with 2% *v/v* HNO_3 prior to MC-ICP-MS measurement.

Mass spectrometry

All isotope measurements were performed using a Thermo Fisher Scientific Neptune Plus MC-ICP-MS. A summary of the typical instrumental parameters is presented in Table 2. Details of the Faraday cup configuration for Sm-Nd isotopic measurements are summarised in Table 3. Compared with the previously reported settings, the sample solution was introduced using an Aridus III desolvator equipped with a self-aspirating 50 µl min^{-1} PFA nebuliser, which reduces H_2O-related interferences and achieves higher sensitivity and stability. To achieve the highest instrument sensitivity during the isotope measurement sessions, an aliquot of a 5 ng g^{-1} isotope standard solution of JNdi-1 Nd or Alfa Sm was regularly used to optimise the operational parameters. The sample introduction system was rinsed with 2% *v/v* HNO_3 to minimise memory effects between each sample measurement. The Nd isotopic data were exported and reduced offline to correct for spike subtraction and instrumental mass bias, using normalisation to $^{146}Nd/^{144}Nd$ = 0.7219 (O'Nions *et al.* 1977) via the exponential law (Russell *et al.* 1978). Meanwhile, Sm and

Table 2.
Typical operating parameters for Sm and Nd isotopic measurement using Neptune Plus MC-ICP-MS + Aridus instrumentation

Parameter	Value
Neptune Plus MC-ICP-MS	
RF forward power	1250 W
Cooling gas	16 l min^{-1}
Auxiliary gas	0.8 l min^{-1}
Sample gas	~1.00 l min^{-1} (optimised daily)
Extraction	-2000 V
Focus	-656 V
Detection system	Nine Faraday collectors
Acceleration voltage	10 kV
Interface cones	Jet sample cone + X skimmer cone
Nebuliser type	Micromist PFA nebuliser
Sample uptake rate	50 µl min^{-1}
Uptake mode	Free aspiration
Instrument resolution	~ 400 (Low)
Typical sensitivity on ^{146}Nd	~ 8 6 V per µg g^{-1} (10^{11} Ω resistors)
Sampling mode	9 blocks of 8 cycles for Nd 1 block of 60 cycles for Sm
Integration time	8 s for Nd and 4 s for Sm
Baseline/background determination	*ca.*1 min on peak in 2% *v/v* HNO_3
Aridus III	
Sweep gas (Ar)	4.3 l min^{-1}
Addition gas (N_2)	3.5 ml min^{-1}
Spray chamber temperature	110 °C
Membrane temperature	160 °C

Table 3.
Faraday cup configuration for Sm and Nd isotopic measurement

Faraday cup	L4	L3	L2	L1	Centre	H1	H2	H3	H4
Measured element	^{144}Sm^{+}	^{146}Nd^{+}	**^{147}Sm^{+}**	^{148}Sm^{+}	Sm **^{149}Sm^{+}**	^{150}Sm^{+}	^{152}Sm^{+}	^{154}Sm^{+}	^{155}Gd^{+}
Interference element	^{144}Nd^{+}			^{148}Nd^{+}		^{150}Nd^{+}	^{152}Gd^{+}	^{154}Gd^{+}	
Measured element	^{142}Nd^{+}	^{143}Nd^{+}	**^{144}Nd^{+}**	^{145}Nd^{+}	Nd **^{146}Nd^{+}**		^{148}Nd^{+}		^{150}Nd^{+}
Interference element	^{142}Ce^{+}		^{144}Sm^{+}			^{147}Sm^{+}	^{148}Sm^{+}	^{149}Sm^{+}	^{150}Sm^{+}

Bold text indicates masses used to determine mass fractionation.

Table 4.
Comparison of ^{147}Sm/^{144}Nd and ^{143}Nd/^{144}Nd ratios for BCR-2, GSR-2 and GSR-3 between various methods

Sm (µg g^{-1})	Nd (µg g^{-1})	^{147}Sm /^{144}Nd	^{143}Nd/^{144}Nd (± 2*s*)	Method	Remarks [Instrument]	Reference
BCR-2 (Basalt)						
6.470	28.30	0.1382	0.512636 (07)	Nd^{+}	SIS [S+H cone, Neptune Plus]	This study
6.530	28.31	0.1394	0.512644 (07)	Nd^{+}	Aridus [Jet+X cone, Neptune Plus]	This study
6.580	28.69	0.1387	0.512635 (23)	NdO^{+}	TaF$_5$ [W filament, Isoprobe T]	Chu *et al.* (2019)
6.561	28.74	0.1380	0.512641 (30)	NdO^{+}	TaF$_5$ [W filament, Isoprobe T]	Chu *et al.* (2014a)
6.543	28.60	0.1383	0.512641 (18)	NdO^{+}	TaF$_5$ [W filament, Isoprobe T]	Chu *et al.* (2009)
			0.512616 (11)	NdO^{+}	Si-gel+H$_3$PO$_4$ [W filament, MAT262]	Li *et al.* (2007)
6.612	28.97	0.1380	0.512640 (08)	Nd^{+}	H$_3$PO$_4$ [Re filament, MAT262]	Yang *et al.* (2010b)
6.507	28.44	0.1383	0.512642 (22)	Nd^{+}	SIS [S+H cone, Neptune]	Yang *et al.* (2011)
6.547	28.26	0.1398	0.512635 (29)			Jochum *et al.* (2016)
GSR-2 (Andesite)						
3.217	17.61	0.1105	0.512394 (06)	Nd^{+}	Aridus [Jet+X cone, Neptune Plus]	This study
3.270	17.91	0.1101	0.512393 (12)	Nd^{+}	SIS [S+H cone, Neptune Plus]	This study
3.200	17.60	0.1099	0.512395 (08)	Nd^{+}	SIS [S+H cone, Neptune Plus]	Yang *et al.* (2022)
			0.512382 (10)	Nd^{+}	SIS [S+H cone, Neptune Plus]	Yang *et al.* (2020)
GSR-3 (Basalt)						
9.913	49.76	0.1205	0.512909 (09)	Nd^{+}	SIS [S+H cone, Neptune Plus]	This study
9.886	49.80	0.1200	0.512904 (08)	Nd^{+}	SIS [S+H cone, Neptune Plus]	This study
9.956	49.77	0.1209	0.512908 (08)	Nd^{+}	Aridus [Jet+X cone, Neptune Plus]	This study
			0.512899 (09)	Nd^{+}	Aridus [Nu II]	Bao *et al.* (2018)
			0.512901 (11)	Nd^{+}	DSN-100 [Nu II]	Fourny *et al.* (2016)

NdO^{+} means measurement by TIMS, Nd^{+} means measurement by TIMS or MC-ICP-MS.

Nd mass fractions were calculated from the corrected ^{147}Sm/^{149}Sm and ^{150}Nd/^{144}Nd mixture ratios, respectively, using the isotope dilution equation. All geological sample isotope ratio data are reported after normalising measurement results of the JNdi-1 standard solution to the reference value of ^{143}Nd/^{144}Nd = 0.512115 (Tanaka *et al.* 2000).

For Nd isotope dilution measurements, the raw data were exported and reduced offline to correct for instrumental mass bias and tracer contributions. Nd mass fractions were calculated from the fractionation corrected ^{150}Nd/^{144}Nd mixture ratio using the isotope dilution equation. Data reduction was performed using a self-written MS Excel VBA (Visual Basic for Applications) macro program that incorporates interference corrections and spike subtractions, followed by mass fractionation correction based on the exponential law; these calculations were performed cycle by cycle. For the Sm isotopic measurements, the measurements consisted of one block of forty 4-s cycles. The ^{147}Sm/^{149}Sm ratio for the spiked samples was externally corrected for instrumental mass fractionation by measuring an Alfa Sm calibration solution after every five samples (^{147}Sm/^{149}Sm = 1.08680, Isnard *et al.* 2005). The Sm mass fraction of the sample was then calculated from the corrected ^{147}Sm/^{149}Sm ratio using the isotope dilution equation. For the final Sm, Nd mass fractions and ^{143}Nd/^{144}Nd ratio data set for each RM, the standard deviation at the 95% confidence level (2*s*) of the mean is given as an estimate of data intermediate precision.

During the data collection period, reference materials BCR-2, GSR-2 and GSR-3 were also analysed sequentially

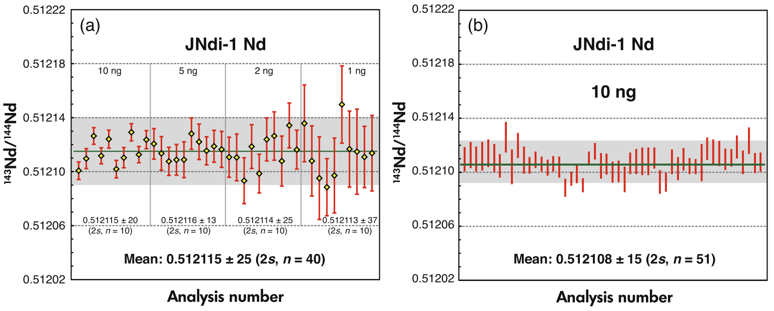

Figure 1. **^{143}Nd/^{144}Nd ratios for different load sizes of JNdi-1 measured using a Neptune Plus MC-ICP-MS equipped with an Aridus III desolvating nebuliser and an X-skimmer cone. Bars on each data point represent 1SE. The solid horizontal line and shaded area indicate the mean and 2*s* of all measurements, respectively.**

using the standard introduction system (SIS) and the Aridus III desolvator (Table 4). Through ten-fold dilution tests of these RMs, the ^{143}Nd/^{144}Nd measurement results obtained using the Aridus III desolvator for BCR-2, GSR-2 and GSR-3 were 0.512644 ± 0.000007 (2*s*), 0.512394 ± 0.000006 (2*s*) and 0.512908 ± 0.000008 (2*s*), respectively. These results are identical to those obtained using the SIS and other methods (Weis *et al.* 2006, Li *et al.* 2007, Chu *et al.* 2009, 2014a, 2019, Yang *et al.* 2010a, 2010b, 2020, Fourny *et al.* 2016, Jochum *et al.* 2016, Wang *et al.* 2017, Guan *et al.* 2019).

Results and discussion

Nd isotopic measurement of trace amounts of Nd

To demonstrate the enhanced capability of the high-sensitivity Neptune Plus MC-ICP-MS coupled with the Aridus III desolvator over the standard wet inlet introduction system, we repeatedly measured the JNdi-1 Nd standard with decreasing sample amounts from 10 to 1 ng of Nd. Normally, a signal intensity of 2–3 V is obtained on ^{146}Nd for a 20 ng g^{-1} Nd solution, assuming that the sample gas flow and ion beam are carefully optimised (Yang *et al.* 2011). The current Nd sensitivity was about ten to fifteen times higher than that of the standard wet inlet introduction system. The mean ^{143}Nd/^{144}Nd ratios for 10 and 5 ng JNdi-1 Nd solutions (i.e., 20 and 10 ng g^{-1} Nd) are 0.512115 ± 0.000020 (2*s*, *n* = 10) and 0.512116 ± 0.000013 (2*s*, *n* = 10), respectively (Figure 1). Comparatively, the mean ^{143}Nd/^{144}Nd ratios for 2 and 1 ng JNdi-1 Nd solutions (i.e., 4 and 2 ng g^{-1} Nd) are 0.512114 ± 0.000025 (2*s*, *n* = 10) and 0.512113 ± 0.000037 (2*s*, *n* = 10), respectively, which are in good agreement with the reference value of 0.512115 (Tanaka *et al.* 2000, Huang *et al.* 2012). The internal ^{143}Nd/^{144}Nd precision varied from 15 to 20 ppm (2SE) for 2 ng Nd and from 35 to 40 ppm (2SE) for 1 ng Nd. These results are in excellent agreement with those previously obtained using the NdO^{+} TIMS technique (~ 5 ng; Li *et al.* 2007, Chu *et al.* 2009, 2014a) or MC-ICP-MS with a wet-method spray chamber and PFA self-aspirating nebuliser (~ 100 ng; Yang *et al.* 2011).

Sample decomposition

Mixtures of HF with HNO_3 or $HClO_4$, as well as similar acid combinations, are commonly used to dissolve silicates in geological samples. Utilising high-purity HF and HNO_3 reduces blank levels. These acids can be readily purchased in highly pure form or produced by repeated sub-boiling distillation of lower-grade acids, which is the method we adopted here. However, in HF-assisted digestion, the formation of insoluble magnesium fluoride (mainly MgF_2) is undesirable, as it significantly reduces the recovery of Sm and Nd. Since typical peridotites contain more than *w* = 35% MgO, such samples are highly prone to forming insoluble fluorides. Although fluorides can generally be decomposed by $HClO_4$, this process is notably inefficient and time-consuming when applied to ultramafic rocks (Sun *et al.* 2013). H_3BO_3 completely dissolves these salts, and solutions with no residue were obtained for the ultra-low abundance geological reference materials analysed in this study. This ensured complete sample digestion and high Sm and Nd recovery yields (Chu *et al.* 2009, 2014a, Ma *et al.* 2019, 2023).

Chemical purification

High-precision measurements of Sm and Nd using the isotope dilution MC-ICP-MS technique require that the analytes be free from matrix elements. After dissolution, the analytes were quantitatively separated from major and trace elements using a single-stage DGA extraction chromatography. Given the extremely high distribution coefficients of rare earth elements (REEs) on DGA resin for most lanthanides, these significant differences in affinity make DGA resin an ideal medium for separating these elements from the rock matrix (Pourmand *et al.* 2012). A novel single-column separation protocol employing DGA resin for (Sr)–Sm–Nd isolation has recently been developed through TIMS method (Chu *et al.* 2019, Xu *et al.* 2024). However, this required stricter control of matrix effects (e.g., residual Ca, Mg) and isotopic fractionation during elution to meet the higher sensitivity and stability demands of MC-ICP-MS.

In this study, we have established an improved chemical procedure based on a single-stage separation between Sm–Nd fractions and the major matrix components. After eluting the major matrix elements and removing most of the La, Ce and Pr, the Nd fraction can be eluted using 2.5 mol l^{-1} HCl, and the Sm fraction is subsequently stripped with 1 mol l^{-1} HCl, achieving high purification. The final Nd fraction matches the purity of the isotope standard Nd solution, indicating complete separation of Sm from Nd and a negligible isobaric interference correction of ^{144}Sm on ^{144}Nd, thereby simplifying the chemical procedure. Our experience indicates that residual Sm is not evident in the Nd fraction, particularly in ultra-low Nd abundance samples (e.g., DTS-2b, JP-1, NIM-D, etc.).

Recovery and total procedural blanks

Regarding the recovery of analytes, a comparison of Nd and Sm mass fractions in the geological RMs with the sample mass reveals that the chemical recovery of Nd and Sm using our procedure was higher than 95%. Besides achieving a high yield of analytes, maintaining a low total procedural blank level is another prerequisite for obtaining reliable Sm-Nd isotopic data for low Nd samples. A Savillex DST-1000 PFA sub-boiling distillation system was used to double-distil the HCl, HF and HNO_3 reagents employed in this work, and sample preparation was conducted within a class 100 clean room environment. The typical total procedural blank values of Sm and Nd – including sample digestion and column chemistry – were less than 5 pg and 10 pg, respectively, which are at the lower end of recently published results (Pin and Zalduegui 1997, Li *et al.* 2007, Chu *et al.* 2009, 2014a, Ali and Srinivasan 2011, Yang *et al.* 2010b, 2011). The total procedural blank contribution in this work is negligible and requires no correction of the measured isotopic ratios and the calculated mass fractions of Sm and Nd.

Precision of the measurement results

To assess the effectiveness of the present protocol, various reference materials from USGS, CCRMP, CNRS, GSJ, IAG and NRC-CRM were used to compare our Sm-Nd mass fraction and isotope ratio measurement results with certified or literature data. Considering the potential heterogeneity of natural geological samples, three to six separate aliquots of RM rock powders were processed using our single chemical procedure (see Table 5). The intermediate precision can be used as an approximate estimate of the measurement uncertainty (Linsinger 2010), assuming that no obvious systematic errors are present in the calibration process. Our measurement results of the RMs, along with certified values and data reported in the literature, are summarised in Tables 6 and 7 for comparison. Method performance was evaluated by comparing the absolute difference (Δ_m) with its expanded uncertainty (U_Δ). When $\Delta_m \le U_\Delta$, this criterion indicates that no statistically significant difference exists between the measured result and the certified value or literature-reported data at the 95% confidence level (Linsinger 2010).

As shown in Table 6, the measurement results for Sm and Nd mass fractions and ^{143}Nd/^{144}Nd ratios of WPR-1a, NIM-N, NIM-P, MUH-1 and JP-1 are consistent with certified values or previously published data within measurement uncertainty, obtained using NdO^+ ID-TIMS and ICP-MS (Figures 2–4; Chu *et al.* 2009, 2014a, Li *et al.* 2011, Fourny *et al.* 2016, IAG 2016a). Specifically, the Sm and Nd mass fractions agree within 2%, and the ^{143}Nd/^{144}Nd values agree within 50 ppm while systematically fulfilling $\Delta_m < U_\Delta$ (Table 7). Some of the Sm and Nd replicate mass fraction data compared with published data (e.g., NIM-D) show differences ($\Delta_m > U_\Delta$) reaching approximately 50% (Figures 2g and 3f; Table 7). This systematic bias is likely attributable to the comparatively high procedural blanks introduced by the Na_2O_2 alkaline-fusion digestion used in the earlier study, which can systematically overestimate REE mass fractions (Kleinhanns *et al.* 2002, Sun and Sun 2009). However, the replicate ^{147}Sm/^{144}Nd ratios for NIM-D agreed within 1.2% of each other (Figure 4b). The other Sm and Nd replicate mass fraction data (e.g., OKUM, DZE-1 and DZE-2) were in excellent agreement with each other, with intermediate precision less than 5% RSD (Figures 2 and 3). The repeatability precision of the ^{143}Nd/^{144}Nd measurement precision for these reference materials was better than 15 ppm, calculated from the mean of nine blocks with ten cycles (Table 5). However, for OKUM, the Sm and Nd mass fractions were slightly lower than the IAG-certified values (Figures 2c and 3b; Tables 6 and 7; IAG 2016b). The cause of this discrepancy is not yet

Table 5.
Measurement results of Sm and Nd mass fractions with ^{143}Nd/^{144}Nd and optional ^{176}Hf/^{177}Hf ratios for ultra-low abundance geological RMs

Sample	MgO (%)	Sm (ng g^{-1})	Nd (ng g^{-1})	^{147}Sm/^{144}Nd	^{143}Nd/^{144}Nd (±2s)$^{\&}$	^{176}Hf/^{177}Hf (±2*s*)
WPR-1a	31	798.2	3140	0.1537	0.512765 (04)	
		807.5	3185	0.1533	0.512757 (05)	
		800.1	3147	0.1537	0.512753 (05)	
		841.6	3347	0.1520	0.512738 (08)	
		843.5	3275	0.1541	0.512762 (08)	
		822.9	3186	0.1562	0.512767 (12)	
Mean [±2*s*]		819.0 [40.5]	3213 [162]	0.1538 [0.0027]	0.512757 [21]	
NIM-N	7.5	819.4	3190	0.1553	0.511750 (07)	
		819.1	3177	0.1558	0.511760 (08)	
		818.8	3185	0.1554	0.511732 (16)	
		813.8	3202	0.1536	0.511752 (08)	
Mean [±2*s*]		817.8 [5.3]	3189 [21]	0.1550 [0.0019]	0.511749 [24]	
NIM-P	25.33	430.0	1948	0.1334	0.511481 (06)	
		428.6	1928	0.1343	0.511495 (06)	
		424.0	1907	0.1343	0.511481 (21)	
		421.0	1926	0.1321	0.511480 (08)	
Mean [±2*s*]		425.9 [8.3]	1927 [33]	0.1336 [0.0022]	0.511484 [14]	
OKUM	21.29	684.9	1452	0.2854	0.514308 (11)	
		688.9	1455	0.2863	0.514303 (10)	
		690.9	1460	0.2862	0.514299 (11)	
Mean [±2*s*]		688.2 [6.1]	1456 [8]	0.2859 [0.0010]	0.514304 [09]	
UB-N	35.21	199.0	558.7	0.2153	0.512903 (12)	
		200.0	572.0	0.2114	0.512933 (06)	
		200.6	570.9	0.2124	0.512916 (06)	
		206.9	576.6	0.2170	0.512927 (06)	
		207.3	576.7	0.2173	0.512930 (07)	
		206.8	573.5	0.2180	0.512944 (08)	
Mean [±2*s*]		203.4 [7.9]	571.4 [13.3]	0.2153 [0.0055]	0.512926 [29]	
HARZ01	45.84				0.511828 (17)	
		1.53	196.8	0.00471	0.511860 (17)	
		1.71	199.9	0.00517	0.511847 (13)	
		1.30	227.2	0.00346	0.511887 (08)	
		1.55	245.7	0.00381	0.511876 (22)	0.282379 (17)
Mean [±2*s*]		1.52 [0.34]	217.4 [46.6]	0.00429 [0.00158]	0.511860 [47]	
MUH-1	38.25	62.8	166.2	0.2283	0.512947 (29)	
					0.512899 (15)	
		65.0	169.2	0.2321	0.512904 (16)	
		65.2	169.7	0.2323	0.512943 (13)	
		64.1	168.9	0.2284	0.512890 (24)	0.283624 (17)
Mean [±2*s*]		64.4 [2.2]	168.7 [4.5]	0.2303 [0.0044]	0.512916 [53]	
DZE-2	38.34	22.9	126.1	0.1096	0.512226 (17)	
		22.1	122.7	0.1087	0.512227 (17)	
		24.7	131.8	0.1132	0.512234 (17)	
Mean [±2*s*]		23.2 [2.7]	126.9 [9.2]	0.1105 [0.0047]	0.512229 [09]	
DZE-1	41.03				0.511820 (24)	
		17.4	114.9	0.0916	0.511820 (26)	
		17.1	121.4	0.0853	0.511755 (20)	
Mean [±2*s*]		17.3 [0.4]	118.2 [9.3]	0.0884 [0.0089]	0.511798 [75]	
NIM-D	43.51	11.1	52.4	0.128	0.511802 (27)	
		11.5	53.4	0.131	0.511814 (17)	
		12.1	56.7	0.128	0.511756 (12)	
					0.511756 (12)	
		11.7	54.1	0.131	0.511790 (12)	
		11.9	54.4	0.132	0.511829 (14)	
		11.9	55.1	0.130	0.511796 (11)	0.282697 (06)
Mean [±2*s*]		11.7 [0.7]	54.4 [3.0]	0.130 [0.003]	0.511792 [55]	
JP-1	44.72	7.62	29.8	0.154	0.512611 (34)	
					0.512595 (15)	
		7.95	30.9	0.156	0.512627 (15)	
		8.21	30.9	0.161	0.512596 (19)	
		8.05	30.8	0.158	0.512589 (18)	

Table 5 (continued).
Measurement results of Sm and Nd mass fractions with $^{143}Nd/^{144}Nd$ and optional $^{176}Hf/^{177}Hf$ ratios for ultra-low abundance geological RMs

Sample	MgO (%)	Sm (ng g^{-1})	Nd (ng g^{-1})	$^{147}Sm/^{144}Nd$	$^{143}Nd/^{144}Nd$ ($\pm 2s$)&	$^{176}Hf/^{177}Hf$ ($\pm 2s$)
Mean [±2s]		7.96 [0.50]	30.6 [1.0]	0.157 [0.005]	0.512603 [31]	
DTS-2b	49.4				0.512542 (32)	
		4.06	17.7	0.138	0.512526 (23)	
		3.25	14.4	0.137	0.512530 (36)	
		3.12	13.2	0.142	0.512501 (33)	
Mean [±2s]		3.48 [1.02]	15.1 [4.7]	0.139 [0.006]	0.512525 [35]	

#Approximately 0.05 g (WPR-1a, NIM-N), 0.1 g (NIM-P, OKUM) and 0.2 g (UB-N) aliquots were weighed for experimental procedures. Approximately 0.3 g of HARZ01, MUH-1 and DZE were weighted for digestion, corresponding to about 10 ng of Nd, while 0.5 g of rock power were digested for the NIM-D, JP-1 and DTS-2b, which corresponded to approximately 5 ng, 3 ng and 2 ng of Nd, respectively. The MgO (%) data are from GeoReM (http://georem.mpch-mainz.gwdg.de/) or corresponding certificate data. & The 2s means the standard errors for $^{143}Nd/^{144}Nd$ and $^{176}Hf/^{177}Hf$ are reported as times 10^6.

Table 6.
Compilation of Sm and Nd mass fractions with $^{147}Sm/^{144}Nd$-$^{143}Nd/^{144}Nd$ and $^{176}Hf/^{177}Hf$ ratios of mafic-ultramafic rock reference materials

Sample	Sm [$\pm 2s$] (ng g^{-1})	Nd [$\pm 2s$] (ng g^{-1})	$^{147}Sm/^{144}Nd$ [$\pm 2s$]	$^{143}Nd/^{144}Nd$ [$\pm 2s$]	*n*	$^{176}Hf/^{177}Hf$ [$\pm 2s$]	*n*	Reference
WPR-1a	819.0 [40.5]	3213 [162]	0.1538 [0.0027]	0.512757 [21]	6			This study
	835.0 [42.4]	3320 [113]	0.1522 [0.0025]	0.512764 [04]	2			Li *et al.* (2011)
NIM-N	817.8 [5.3]	3189 [21]	0.1550 [0.0019]	0.511749 [24]	4			This study
	832.5 [67.7]	3170 [256]	0.1568	0.511756 (25)	10			Fourny *et al.* (2016)
NIM-P	425.9 [8.3]	1927 [33]	0.1336 [0.0022]	0.511484 [14]	4			This study
	428.8 [17.8]	1871 [36]	0.1387	0.511501 (07)	3			Fourny *et al.* (2016)
OKUM	688.2 [6.1]	1456 [8]	0.2859 [0.0010]	0.514304 [09]	3			This study
	715 [11]	1494 [20]						Certified value
UB-N	203.4 [7.9]	571.4 [13.3]	0.2153 [0.0055]	0.512926 [29]	6			This study
	212 [2]	592 [5]	0.2167 [0.0009]	0.512950 [26]	4			Chu *et al.* (2019)*
				0.512929 [05]	4			Pin and Gannoun (2019)
	208 [12]	582 [38]			5			Rospabé *et al.* (2018)
	214 [10]	603 [35]	0.2143 [0.0026]	0.512926 [01]	2			Pin and Zalduegui (1997)
				0.512948 [08]	4			Zhou *et al.* (2024)
HARZ01	1.52 [0.34]	217.4 [46.6]	0.00429 [0.00158]	0.511860 [47]	5	0.282379 [17]	1	This study
						0.282368 [44]	9	Ma *et al.* (2023)
						0.282366 [19]	3	Ma *et al.* (2019)
	1.18 [0.39]	219.2 [0.9]					2	Day *et al.* (2016)
MUH-1	64.4 [2.2]	168.7 [4.5]	0.2303 [0.0044]	0.512916 [53]	4	0.283624 [17]	1	This study
	65.1 [0.4]	174.0 [1.4]	0.2267 [0.0033]	0.512966 [13]	2			Chu *et al.* (2019)*
	67.7 [2.6]	177.0 [7.0]						Certified value
DZE-2	23.2 [2.7]	126.9 [9.2]	0.1105 [0.0047]	0.512229 [09]	3			This study
	28.0 [2.8]	150 [14]			5			Sun and Sun (2009)
	23.2 [2.8]	131 [22]			4			Qi *et al.* (2005)
DZE-1	17.3 [0.4]	118.2 [9.3]	0.0884 [0.0089]	0.511798 [75]	3			This study
	21.1 [4.0]	128 [14]			5			Sun and Sun (2009)
	19.9 [3.6]	119 [12]			5			Qi *et al.* (2005)
NIM-D	11.7 [0.7]	54.4 [3.0]	0.130 [0.003]	0.511792 [55]	6	0.282697 [06]	1	This study
						0.282730 [54]	9	Ma *et al.* (2023)
						0.282726 [20]	3	Ma *et al.* (2019)
	20.8 [3.0]	82.3 [4.0]			4			Sun and Sun (2009)
JP-1	7.96 [0.50]	30.6 [1.0]	0.157 [0.005]	0.512603 [31]	5			This study
	7.39 [0.90]	29.6 [3.3]			5			Rospabé *et al.* (2018)
	7.96 [0.29]	31.2 [1.2]	0.154 [0.002]	0.512637 [34]	5			Chu *et al.* (2014a)*
	7.76 [0.80]	34.7 [3.2]			5			Sun *et al.* (2013)
	7.69 [0.40]	29.7 [3.0]			5			Qi *et al.* (2005)
DTS-2b	3.48 [1.02]	15.1 [4.7]	0.139 [0.006]	0.512525 [35]	4			This study
	2.81 [0.32]	13.1 [2.4]			10			Rospabé *et al.* (2018)
	3.00 [0.14]	13.2 [0.8]	0.137 [0.004]	0.512542 [59]	5			Chu *et al.* (2014a)*

The 2*s* means the standard deviation and are reported as times 10^6 for $^{143}Nd/^{144}Nd$ and $^{176}Hf/^{177}Hf$.

* means NdO^+ measurement by TIMS, others mean Nd^+ measurement by TIMS or MC-ICP-MS.

Table 7.
Comparative evaluation of Sm-Nd mass fraction and $^{143}Nd/^{144}Nd$ ratio uncertainties in mafic-ultramafic rock reference materials

Sample	Sm [±2*s*] (ng g^{-1})	Δ_m (U_Δ) (ng g^{-1})	Nd [±2*s*] (ng g^{-1})	Δ_m (U_Δ) (ng g^{-1})	$^{143}Nd/^{144}Nd$ [±2*s*]	*n*	Δ_m (U_Δ)	Reference
WPR-1a	819.0 [40.5]		3213 [162]		0.512757 [21]	6		This study
	835.0 [42.4]	16.0 (<58.6)	3320 [113]	107 (<198)	0.512764 [04]	2	7 (<22)	Li *et al.* (2011)
NIM-N	817.8 [5.3]		3189 [21]		0.511749 [24]	4		This study
	832.5 [67.7]	14.8 (<67.9)	3170 [256]	18 (<257)	0.511756 [50]	10	8 (<55)	Fourny *et al.* (2016)
NIM-P	425.9 [8.3]		1927 [33]		0.511484 [14]	4		This study
	428.8 [17.8]	2.9 (<19.6)	1871 [36]	57 (> 49)	0.511501 [07]	3	17 (<20)	Fourny *et al.* (2016)
OKUM	688.2 [6.1]		1456 [8]		0.514304 [09]	3		This study
	715 [11]	26.8 (> 12.6)	1494 [20]	38 (> 22)				Certified value
UB-N	203.4 [7.9]		571.4 [13.3]		0.512926 [29]	6		This study
	212 [2]	8.6 (> 8.1)	592 [5]	20.6 (> 14.3)	0.512950 [26]	4	24 (<38)	Chu *et al.* (2019)
					0.512929 [05]	4	3 (<29)	Pin and Zalduegui (2019)
	208 [12]	4.6 (<14.4)	582 [38]	10.6 (<40.3)		5		Rospabé *et al.* (2018)
	214 [10]	10.1 (<12.7)	603 [35]	31.1 (<37.8)	0.512926 [01]	2	0 (<29)	Pin and Zalduegui (1997)
					0.512948 [08]	4	22 (<30)	Zhou *et al.* (2024)
HARZ01	1.52 [0.34]		217.4 [46.6]		0.511860 [47]	5		This study
	1.18 [0.39]	0.34 (<0.51)	219.2 [0.9]	1.8 (<46.6)				Day *et al.* (2016)
			218.5 [40.6]	1.1 (<61.8)		44		Webb *et al.* (2016)
MUH-1	64.4 [2.2]		168.7 [4.5]		0.512916 [53]	4		This study
	65.1 [0.4]	0.8 (<2.2)	174.0 [1.4]	5.3 (> 4.7)	0.512966 [13]	2	49 (<54)	Chu *et al.* (2019)
	67.7 [2.6]	3.4 (=3.4)	177.0 [7.0]	8.3 (=8.3)				Certified value
DZE-2	23.2 [2.7]		126.9 [9.2]		0.512229 [09]	3		This study
	28.0 [2.8]	4.8 (> 3.9)	150 [14]	23.1 (> 16.8)		5		Sun and Sun (2009)
	23.2 [2.8]	0 (<3.9)	131 [22]	4.1 (<23.8)		4		Qi *et al.* (2005)
DZE-1	17.3 [0.4]		118.2 [9.3]		0.511798 [75]	3		This study
	21.1 [4.0]	3.9 (<4.0)	128 [14]	9.8 (<16.8)		5		Sun and Sun (2009)
	19.9 [3.6]	2.7 (<3.6)	119 [12]	0.8 (<15.2)		5		Qi *et al.* (2005)
NIM-D	11.7 [0.7]		54.4 [3.0]		0.511792 [55]	6		This study
	20.8 [3.0]	9.1 (> 3.1)	82.3 [4.0]	28.0 (> 5.0)		4		Sun and Sun (2009)
JP-1	7.96 [0.50]		30.6 [1.0]		0.512603 [31]	5		This study
	7.39 [0.90]	0.57 (<1.03)	29.6 [3.3]	1.0 (<3.5)		5		Rospabé *et al.* (2018)
	7.96 [0.29]	0 (<0.57)	31.2 [1.2]	0.6 (<1.6)	0.512637 [34]	5	34 (<46)	Chu *et al.* (2014a)
	7.76 [0.80]	0.20 (<0.94)	34.7 [3.2]	4.1 (> 3.4)		5		Sun *et al.* (2013)
	7.69 [0.40]	0.27 (<0.64)	29.7 [3.0]	0.9 (<3.2)		5		Qi *et al.* (2005)
DTS-2b	3.48 [1.02]		15.1 [4.7]		0.512525 [35]	4		This study
	2.81 [0.32]	0.67 (<1.07)	13.1 [2.4]	2.0 (<5.2)		10		Rospabé *et al.* (2018)
	3.00 [0.14]	0.48 (<1.03)	13.2 [0.8]	1.9 (<4.7)	0.512542 [59]	5	17 (<68)	Chu *et al.* (2014a)

Δ_m means absolute difference between mean measured value and certified/literature value (Linsinger 2010).

U_Δ means expanded uncertainty of difference between result and certified/literature value (Linsinger 2010).

Δ_m (U_Δ) of $^{143}Nd/^{144}Nd$ ratios are reported as times 10^6.

OKUM and MUH-1 were compared with certified reference values; others were benchmarked against literature-reported data from recent studies (uncertified values).

fully understood. The digestion aliquot used in our study was 100 mg, which is below the recommended minimum test portion of 200 mg specified in the certificate of analysis (IAG 2016b). In our study, we performed three replicates for OKUM, and all results were consistently lower than the certified values, indicating a systematic issue rather than one stemming from random heterogeneity (Table 5). The Sm/Nd ratio we obtained was 0.4727, which shows only a 1.2% deviation compared with the certified value of 0.4786. Currently, there is no available data based on isotope dilution methods, and existing reports primarily rely on LA-ICP-MS or solution ICP-MS measurements (Peters and Pettke 2017, Waterton *et al.* 2017). Therefore, we speculate that the certified value might have a smaller assigned uncertainty, or that other unknown factors may be involved that could explain the discrepancy. Additionally, the obtained mass fraction and isotopic data we obtained for UB-N show excellent agreement with previously reported measurement results from ID-TIMS and MC-ICP-MS (Figures 2d, 3c and 4e; Pin and Zalduegui 1997, Pin and Gannoun 2019, Chu *et al.* 2019, Zhou *et al.* 2024). For HARZ01, while the Sm and Nd mass fraction data from four

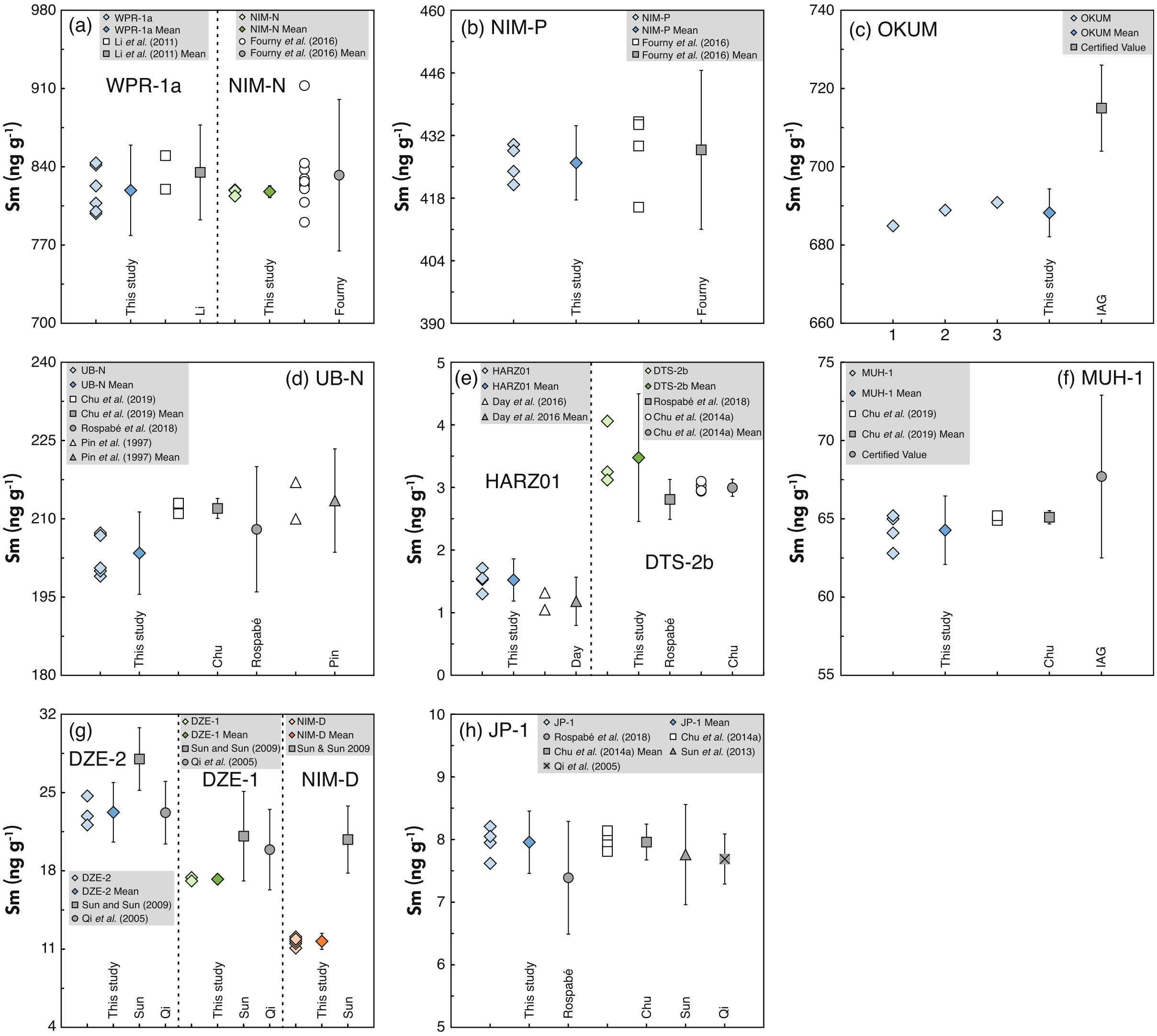

Figure 2. Samarium mass fractions in mafic-ultramafic rock RMs compared with published values. The graphical configuration systematically follows the tabulated order in Table 5 and employs mass fraction-dependent clustering (Sm ± 10 ng g^{-1}). Bars on each sample data point represent 2*s*.

duplicate samples demonstrated a relative standard deviation of approximately 10%, their mean values align closely with previously published data - particularly in Nd mass fraction (217.4 ± 46.6 ng g^{-1}) showing merely 0.5% deviation from the Geo*PT*38A certified value (218.5 ± 40.6 ng g^{-1}) (Figures 2e and 3d; Table 7; Webb *et al.* 2016). DTS-2b, which has the lowest Nd mass fraction among the ultramafic rock RMs measured in this study, showed more variable Sm and Nd mass fractions than those obtained by the NdO$^+$ ID-TIMS method, although the test portion sizes differed between the two analytical approaches (500 mg for ID-MC-ICP-MS *vs.* 300 mg for ID-TIMS) (Figures 2e and 3h; Chu *et al.* 2014a).

Advantages of the measurement procedure

Regarding samples with relatively low Nd mass fraction, it is well known that Nd can be ionised more efficiently as NdO$^+$ than as Nd$^+$ on TIMS. The high-sensitivity NdO$^+$ TIMS technique is still regarded as the benchmark for measurement of trace amounts of Nd isotopes (Thirlwall *et al.* 1991, Griselin *et al.* 2001, Li *et al.* 2007, Chu *et al.* 2009, 2014a, Harvey and Baxter 2009). Nevertheless, it is well recognised that a lengthy and tedious chromatographic separation of Nd from not only Sm (^{144}SmO$^+$ on ^{144}NdO$^+$) but also Ce and Pr is required due to isobaric interferences of CeO$^+$ and PrO$^+$ on NdO$^+$. Previously reported procedures for Nd

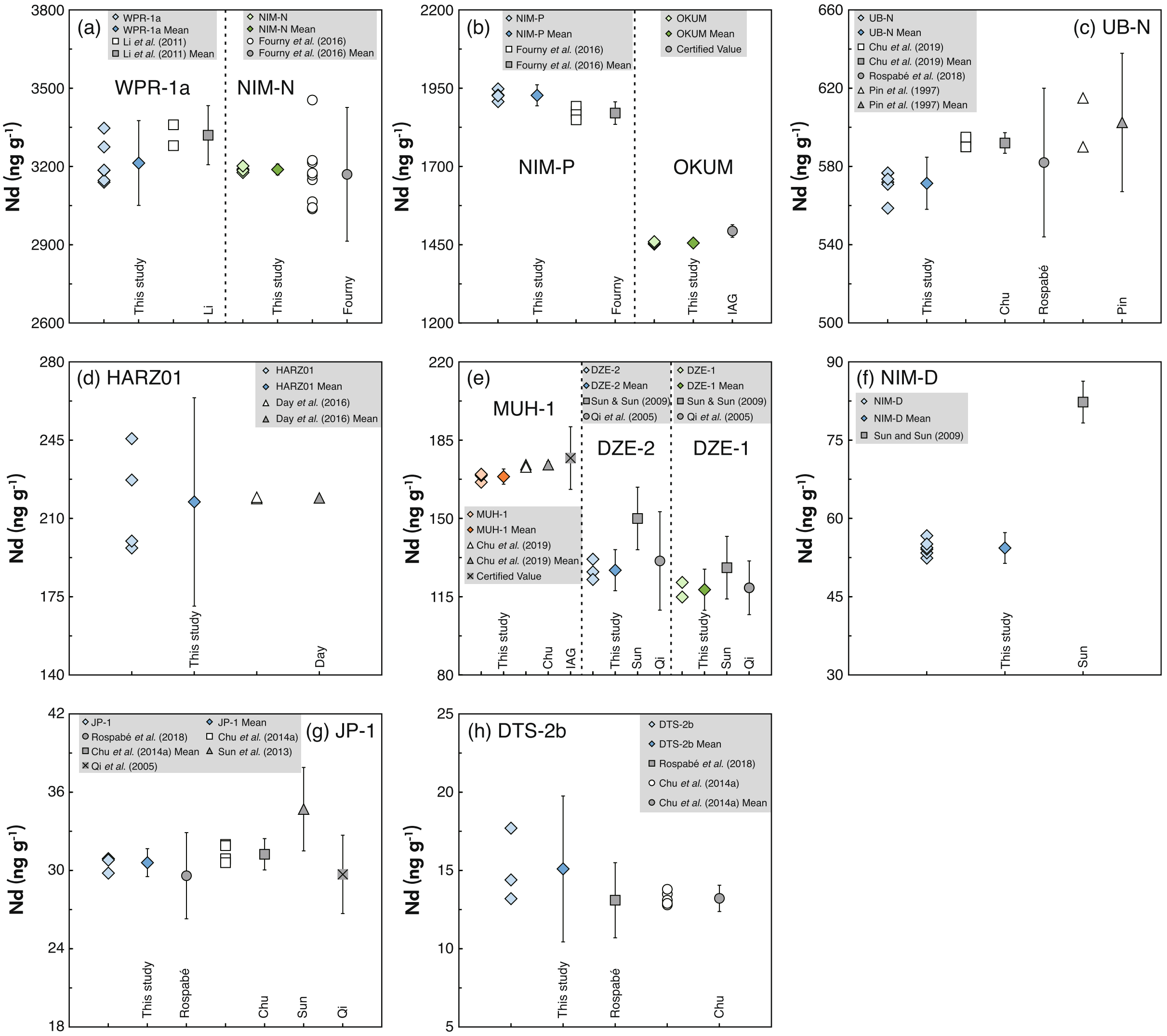

Figure 3. Neodymium mass fractions in mafic-ultramafic rock RMs compared with published values. The graphical configuration systematically follows the tabulated order in Table 5, with specimens exhibiting comparable Nd mass fractions (RSD < 15%) grouped within individual panels. Bars on each sample data point represent 2*s*.

extraction from rock samples for NdO^+ measurement include high-pressure liquid chromatography (HPLC) and α-hydroxyisobutyric acid (HIBA) chromatography. Both techniques can achieve highly efficient separation of the individual REE but are inconvenient for practical application and require special equipment and rigorous experimental conditions. Therefore, chemical isolation is associated with at least two or even three stages of column chromatography, as well as lower yields of Sm and Nd analytes (e.g., ~ 70%) (Griselin *et al.* 2001, Li *et al.* 2007, Chu *et al.* 2009, 2014a).

In mass spectrometric measurements, loading the purified Sm or Nd fractions onto single or triple pre-degassed filaments usually requires several hours of analytical time. Moreover, TIMS typically takes 3–4 h to evacuate the thermal ionisation source following the exchange of the sample magazine. Additionally, uncertainties arise from oxygen corrections (i.e., the reduction of NdO^+ isotopic ratios to Nd isotopic ratios) (Amelin 2004, Li *et al.* 2007, Chu *et al.* 2009, 2014a, Harvey and Baxter 2009). In summary, the NdO^+ method can be more dependent on the technician's analytical experience. Furthermore, its relatively low efficiency cannot meet the increasing demand for widespread applications of the Sm–Nd isotopic system in geochemistry and environmental sciences, particularly for samples with low amounts of Sm and Nd. In this study, the chemical purification procedure was reduced from at least two or three stages to a single-

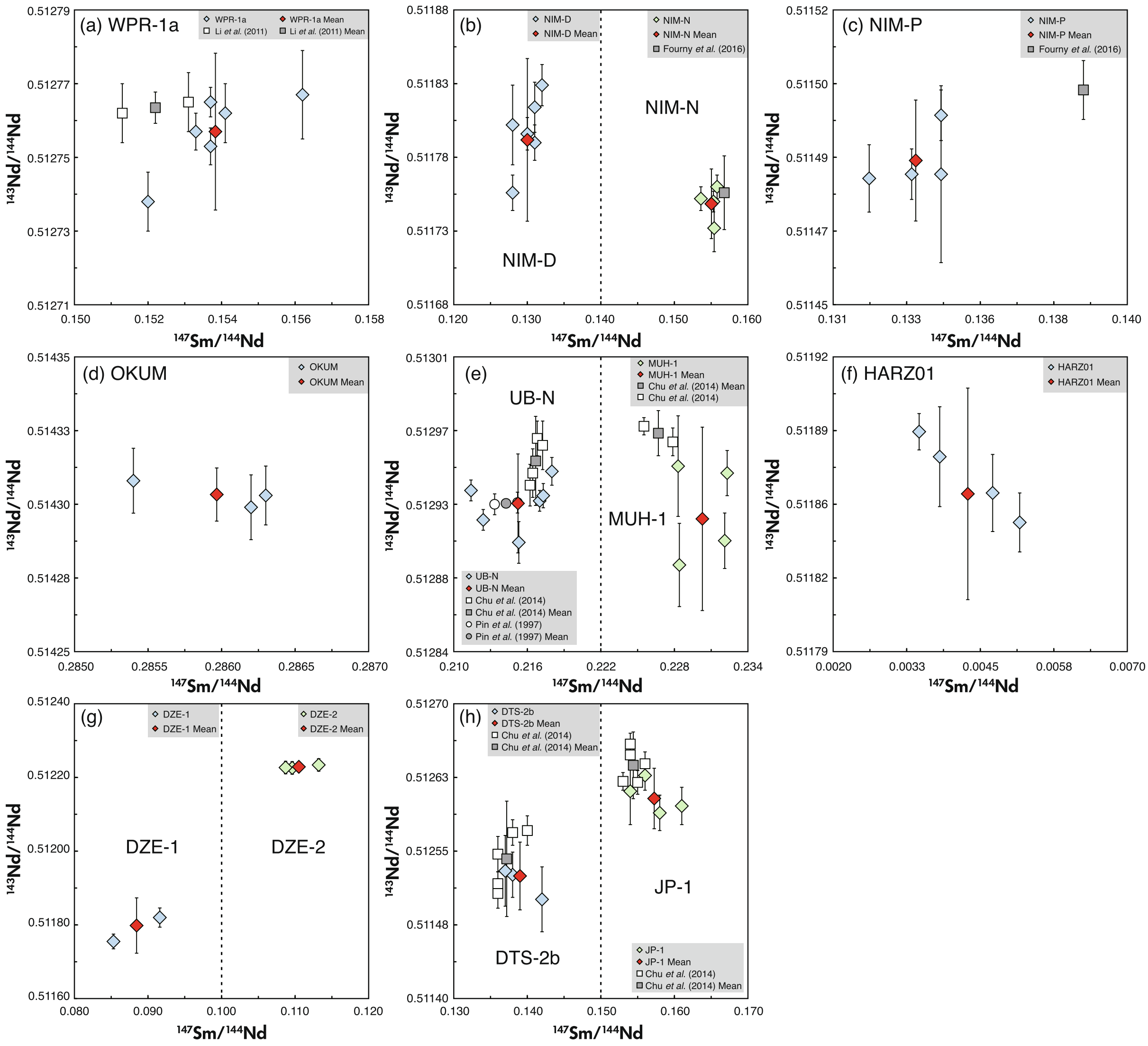

Figure 4. Plots of $^{147}Sm/^{144}Nd$ *vs.* $^{143}Nd/^{144}Nd$ ratios from mafic-ultramafic rock RMs compared with published values. Bars on each data point represent 2SE, while bars for the mean values of each sample represent 2*s*.

stage column chemistry, resulting in reduced contamination and improved efficiency. Compared with classic TIMS, MC-ICP-MS is characterised by its combination of a magnetic sector multi-collector Faraday cup array and a highly efficient ICP ion source, which makes high-precision isotope measurements and high sample throughput possible. With the integration of new-generation sample inlet systems (e.g., Aridus or Apex) and MC-ICP-MS instruments (e.g., Neptune Plus, Nu Plasma 3), it is becoming feasible to analyse samples with low Nd mass fractions (Huang *et al.* 2012, Zhou *et al.* 2024).

In contrast to NdO^+ TIMS, MC-ICP-MS requires less chemical labour, minimal matrix effects on column chemistry, and is less dependent on technician experience. In terms of simplicity, feasibility and sample throughput for routine measurements of low amounts of Nd isotopes, MC-ICP-MS has obvious advantages over the currently less popular NdO^+ TIMS techniques. First, there is no need for a lengthy chromatographic separation of Nd from not only Sm but also Ce and Pr (Li *et al.* 2007, Chu *et al.* 2009, 2014a). Second, there is no need for complex online oxygen isotope correction, which is typically associated with significant uncertainties arising from the reduction of NdO isotopic ratios to Nd isotopic ratios (Chu *et al.* 2014b). Third, it is unnecessary to consider the technician's experience during mass spectrometric preparation, such as the addition of ionisation activators (e.g., silica gel/H_3PO_4, Ta_2O_5 etc.) and the use of high-purity metal filaments, both of which are prerequisites to enhance signal intensity and stability. The MC-ICP-MS technique demonstrates significant potential for trace Nd isotopic determinations in ultra-low Nd abundance geological samples, further emphasising its efficacy in measuring trace amounts of Nd in natural samples.

Summary and conclusion

In this work, we have developed a simple, rapid and practical measurement procedure for the highly reproducible analysis of Sm and Nd mass fractions and ^{143}Nd/^{144}Nd ratios in mafic-ultramafic geological samples using MC-ICP-MS, without compromising the precision of the measurements. This technique is superior in terms of measurement precision and speed compared with TIMS NdO^{+} techniques. Using the proposed procedure, replicate measurements of ultra-low abundance geological certified and non-certified reference materials demonstrate that Sm and Nd mass fractions can be reproduced with intermediate precision better than 2% RSD, and the measured ^{147}Sm/^{144}Nd and ^{143}Nd/^{144}Nd ratios show no systematic bias ($\Delta_m < U_\Delta$) and are consistent with published values within measurement uncertainty, obtained by TIMS and MC-ICP-MS methods. Moreover, we have provided new Sm–Nd isotopic data for HARZ01, MUH-1, NIM-D, DZE-1 and DZE-2. Given the successful column chemistry and sufficiently low blanks, the described measurement procedure allows low quantification limits never reached before and will offer more opportunities in a wide range of research fields, including geochemistry, cosmochemistry and environmental sciences. Therefore, the high sample throughput inherent to MC-ICP-MS can be fully exploited for the classic Sm–Nd isotopic system.

Acknowledgements

This work was financially supported by the National Natural Science Foundation of China (42430105, 42403029, 42473036 and 42473037) and the State Key Laboratory of Lithospheric and Environmental Coevolution, Institute of Geology and Geophysics, Chinese Academy of Sciences (SKL-Z202304). We are indebted to T.C. Meisel for providing the HARZ01 and MUH-1 samples. We are also grateful to the two anonymous reviewers for their critical and insightful comments, which have significantly improved this manuscript. Researchers interested in contributing data on these samples are welcome to contact us, as we are willing to provide aliquots of these rock reference materials. There are no conflicts of interest to declare.

Scientific editing by Regina Mertz-Kraus.

Data availability statement

Data will be made available upon reasonable request.

References

Ali A. and Srinivasan G. (2011)
Precise thermal ionization mass spectrometric measurements of ^{142}Nd/^{144}Nd and ^{143}Nd/^{144}Nd isotopic ratios of Nd separated from geological standards by chromatographic methods. International Journal of Mass Spectrometry, 299, 27–34.

Amelin Y. (2004)
Sm–Nd systematics of zircon. Chemical Geology, 211, 375–387.

Bao Z.A., Zong C.L., Fang L.R., Yuan H.L., Chen K.Y. and Dai M.N. (2018)
Determination of Hf–Sr–Nd isotopic ratios by MC-ICP-MS using rapid acid digestion after flux-free fusion in geological materials. Acta Geochimica, 37, 244–256.

Bouvier A., Vervoort J.D. and Patchett P.J. (2008)
The Lu–Hf and Sm–Nd isotopic composition of CHUR: Constraints from unequilibrated chondrites and implications for the bulk composition of terrestrial planets. Earth and Planetary Science Letters, 273, 48–57.

Chu Z.Y., Chen F.K., Yang Y.H. and Guo J.H. (2009)
Precise determination of Sm, Nd concentrations and Nd isotopic compositions at the nanogram level in geological samples by thermal ionization mass spectrometry. Journal of Analytical Atomic Spectrometry, 24, 1534–1544.

Chu Z.Y., Guo J.H., Yang Y.H., Qi L. and Li C.F. (2014a)
Precise determination of Sm and Nd concentrations and Nd isotopic compositions in highly depleted ultramafic reference materials. Geostandards and Geoanalytical Research, 38, 61–72.

Chu Z.Y., Li C.F., Hegner E., Chen Z., Yan Y. and Guo J.H. (2014b)
High-precision ^{143}Nd/^{144}Nd ratios from NdO^{+} data corrected with in-run measured oxygen isotope ratios. Analytical Chemistry, 86, 11141–11150.

Chu Z.Y., Wang M.J., Li C.F., Yang Y.H., Xu J.J., Wang W. and Guo J.H. (2019)
Separation of Nd from geological samples by a single TODGA resin column for high precision Nd isotope analysis as NdO^{+} by TIMS. Journal of Analytical Atomic Spectrometry, 34, 2053–2060.

Connelly J.N., Ulfbeck D.G., Thrane K., Bizzarro M. and Housh T. (2006)
A method for purifying Lu and Hf for analyses by MC-ICP-MS using TODGA resin. Chemical Geology, 233, 126–136.

Day J.M.D., Waters C.L., Schaefer B.F., Walker R.J. and Turner S. (2016)
Use of hydrofluoric acid desilicification in the determination of highly siderophile element abundances and Re-Pt-Os isotope systematics in mafic-ultramafic rocks. Geostandards and Geoanalytical Research, 40, 49–65.

references

Dubois J.C., Retali G. and Cesario J. (1992)
Isotopic analysis of rare earth elements by total vaporization of samples in thermal ionization mass spectrometry. International Journal of Mass Spectrometry and Ion Processes, 120, 163–177.

Faure G. and Mensing T.M. (2004)
Isotopes: Principles and applications (3rd edition). Wiley (New Jersey), 928pp.

Foster G.L. and Vance D. (2006)
In situ Nd isotopic analysis of geological materials by laser ablation MC-ICP-MS. Journal of Analytical Atomic Spectrometry, 21, 288–296.

Fourny A., Weis D. and Scoates J.S. (2016)
Comprehensive Pb-Sr-Nd-Hf isotopic, trace element, and mineralogical characterization of mafic to ultramafic rock reference materials. Geochemistry, Geophysics, Geosystems, 17, 739–773.

Garbe-Schonberg D. and Muller S. (2014)
Nano-particulate pressed powder tablets for LA-ICP-MS. Journal of Analytical Atomic Spectrometry, 29, 990–1000.

Griselin M., van Belle J.C., Pomiès C., Vroon P.Z., van Soest M.C. and Davies G.R. (2001)
An improved chromatographic separation technique of Nd with application to NdO^+ isotope analysis. Chemical Geology, 172, 347–359.

Guan Q.Y., Sun Y.L., Yue Y.H., Liu X.M. and Zhao S.Q. (2019)
A simplified method using a single N,N,N′,N′-tetraoctyl diglycolamide resin column for the purification of Sr, Nd and Hf in geological materials and the determination of their isotopic ratios by multi-collector inductively coupled plasma-mass spectrometry. Analytical Sciences, 35, 323–328.

Halliday A.N., Lee D.C., Christensen J.N., Walder A.J., Freedman P.A., Jones C.E., Hall C.M., Yi W. and Teagle D. (1995)
Recent developments in inductively coupled plasma magnetic sector multiple collector mass spectrometry. International Journal of Mass Spectrometry and Ion Processes, 146–147, 21–33.

Harvey J. and Baxter E.F. (2009)
An improved method for TIMS high precision neodymium isotope analysis of very small aliquots (1–10 ng). Chemical Geology, 258, 251–257.

Huang F.K., Blusztajin J., Oppo D.W., Curry W.B. and Peucker-Ehrenbrink B. (2012)
High-precision and accurate determinations of neodymium isotopic compositions at nanogram levels in natural materials by MC-ICP-MS. Journal of Analytical Atomic Spectrometry, 27, 1560–1567.

IAG (2016a)
MUH-1 Certified Reference Material (CRM-5). International Association of Geoanalysts. https://iageo.com/wp-content/uploads/2020/03/MUH-1-Certificate-of-analysis-revised-4th-November-2016.pdf

IAG (2016b)
OKUM Certified Reference Material (CRM-4). International Association of Geoanalysts. https://iageo.com/wp-content/uploads/2020/03/OKUM-Certificate-of-analysis-revised-04Nov2016.pdf

Isnard H., Brennetot R., Caussignac C., Caussignac N. and Chartier F. (2005)
Investigations for determination of Gd and Sm isotopic compositions in spent nuclear fuels samples by MC-ICP-MS. International Journal of Mass Spectrometry, 246, 66–73.

Jochum K.P., Weis U., Schwager B., Stoll B., Wilson S.A., Haug G.H., Andreae M.O. and Enzweiler J. (2016)
Reference values following ISO guidelines for frequently requested rock reference materials. Geostandards and Geoanalytical Research, 40, 333–350.

Kleinhanns I.C., Kreissig K., Kamber B.S., Meisel T., Nägler T.F. and Kramers J.D. (2002)
Combined chemical separation of Lu, Hf, Sm, Nd, and REEs from a single rock digest: Precise and accurate isotope determinations of Lu–Hf and Sm–Nd using multicollector-ICP-MS. Analytical Chemistry, 74, 67–73.

Li C.F., Chen F.K. and Li X.H. (2007)
Precise isotopic measurements of sub-nanogram Nd of standard reference material by thermal ionization mass spectrometry using the NdO^+ technique. International Journal of Mass Spectrometry, 226, 34–41.

Li C.F., Li X.H., Li Q.L., Guo J.H., Li X.H. and Liu T. (2011)
An evaluation of a single-step extraction chromatography separation method for Sm–Nd isotope analysis of micro-samples of silicate rocks by high-sensitivity thermal ionization mass spectrometry. Analytica Chimica Acta, 706, 297–304.

Linsinger T. (2010)
Comparison of a measurement result with the certified value. European Reference Materials (ERM), Application Note 1. https://crm.jrc.ec.europa.eu/graphics/cms_docs/erm1_english.pdf

Lugmair G.W. and Galer S.J.G. (1992)
Age and isotopic relationships among the angrites Lewis Cliff 86010 and Angra dos Reis. Geochimica et Cosmochimica Acta, 56, 1673–1694.

Lugmair G.W. and Marti K. (1978)
Lunar initial $^{143}Nd/^{144}Nd$: Differential evolution of the lunar crust and mantle. Earth and Planetary Science Letters, 39, 349–357.

Ma Q., Yang M., Zhao H., Evans N.J., Chu Z.Y., Xie L.W., Huang C., Zhao Z.D. and Yang Y.H. (2019)
Accurate and precise determination of Lu and Hf mass fractions and Hf isotopic composition at the sub-nanogram level in geological samples using MC-ICP-MS. Journal of Analytical Atomic Spectrometry, 34, 1256–1262.

references

Ma Q., Yang Y.H. and Yang Z.M. (2023)
Determination of Lu and Hf mass fractions and ^{176}Hf/^{177}Hf ratios in mafic-ultramafic rock reference materials by multi-collector inductively coupled plasma-mass spectrometry. Geostandards and Geoanalytical Research, 47, 869–891.

Okina O.I., Lyapunov S.M., Dubenskiy A.S. and Erofeeva K.G. (2020)
An investigation of trace elements' behavior during chemical preparation of ultramafic matrix rock samples using bomb digestion for analysis by ICP-MS. Journal of Analytical Atomic Spectrometry, 35, 2627–2638.

O'Nions R.K., Hamilton P.J. and Evensen N.M. (1977)
Variations in ^{143}Nd/^{144}Nd and ^{87}Sr/^{86}Sr ratios in oceanic basalts. Earth and Planetary Science Letters, 34, 13–22.

Peters D. and Pettke T. (2017)
Evaluation of major to ultra trace element bulk rock chemical analysis of nanoparticulate pressed powder pellets by LA-ICP-MS. Geostandards and Geoanalytical Research, 41, 5–28.

Pin C. and Gannoun A. (2019)
Miniaturized, rapid separation of neodymium from ultramafic and chondritic samples prior to high precision measurements of ^{142,143}Nd/^{144}Nd isotope ratios by TIMS. Journal of Analytical Atomic Spectrometry, 34, 2136–2146.

Pin C. and Zalduegui J.F.S. (1997)
Sequential separation of light rare-earth elements, thorium and uranium by miniaturized extraction chromatography: Application to isotopic analyses of silicate rocks. Analytica Chimica Acta, 339, 79–89.

Pourmand A. and Dauphas N. (2010)
Distribution coefficients of 60 elements on TODGA resin: Application to Ca, Lu, Hf, U and Th isotope geochemistry. Talanta, 81, 741–753.

Pourmand A., Dauphas N. and Ireland T.J. (2012)
A novel extraction chromatography and MC-ICP-MS technique for rapid analysis of REE, Sc and Y: Revising CI-chondrite and Post-Archean Australian Shale (PAAS) abundances. Chemical Geology, 291, 38–54.

Qi L., Zhou M.F., Malpas J. and Sun M. (2005)
Determination of rare earth elements and Y in ultramafic rocks by ICP-MS after preconcentration using Fe(OH)$_3$ and Mg(OH)$_2$ coprecipitation. Geostandards and Geoanalytical Research, 29, 131–141.

Raczek I., Jochum K.P. and Hofmann A.W. (2003)
Neodymium and strontium isotope data for USGS reference materials BCR-1, BCR-2, BHVO-1, BHVO-2, AGV-1, AGV-2, GSP-1, GSP-2 and eight MPI-DING reference glasses. Geostandards Newsletter: The Journal of Geostandards and Geoanalysis, 27, 173–179.

Raczek I., Stoll B., Hofmann A.W. and Jochum K.P. (2001)
High-precision trace element data for the USGS reference materials BCR-1, BCR-2, BHVO-1, BHVO-2, AGV-1, AGV-2, DTS-1, DTS-2, GSP-1 and GSP-2 by ID-TIMS and MIC-SSMS. Geostandards Newsletter: The Journal of Geostandards and Geoanalysis, 25, 77–86.

Retzmann A., Zimmermann T., Pröfrock D., Prohaska T. and Irrgeher J. (2017)
A fully automated simultaneous single-stage separation of Sr, Pb and Nd using DGA Resin for the isotopic analysis of marine sediments. Analytical and Bioanalytical Chemistry, 409, 5463–5480.

Rospabé M., Benoit M. and Candaudap F. (2018)
Determination of trace element mass fractions in ultramafic rocks by HR-ICP-MS: A combined approach using a direct digestion/dilution method and preconcentration by coprecipitation. Geostandards and Geoanalytical Research, 42, 115–129.

Russell W.A., Papanastassiou D.A. and Tombrello T.A. (1978)
Ca isotope fractionation on the Earth and other solar system materials. Geochimica et Cosmochimica Acta, 42, 1075–1090.

Shibata T. and Yoshikawa M.J. (2004)
Precise isotope determination of trace amounts of Nd in magnesium-rich samples. Journal of the Mass Spectrometry Society of Japan, 52, 317–324.

Sun Y.L. and Sun M. (2009)
Determination of ultra-trace rare earth elements in ultramafic and sulfide samples by quadrupole inductively coupled plasma-mass spectrometry. Journal of Analytical Atomic Spectrometry, 24, 232–236.

Sun Y.L., Sun S.L., Wang C.Y. and Xu P. (2013)
Determination of rare earth elements and thorium at nanogram levels in ultramafic samples by inductively coupled plasma-mass spectrometry combined with chemical separation and pre-concentration. Geostandards and Geoanalytical Research, 37, 65–76.

Tanaka T., Togashi S., Kamioka H., Amakawa H., Kagami H., Hamamoto T., Yuhara M., Orihashi Y., Yoneda S., Shimizu H., Kunimaru T., Takahashi K., Yanagi T., Nakano T., Fujimaki H., Shinjo R., Asahara Y., Tanimizu M. and Dragusanu C. (2000)
JNdi-1: A neodymium isotopic reference in consistency with LaJolla neodymium. Chemical Geology, 168, 279–281.

Thirlwall M.F. (1991)
High-precision multicollector isotopic analysis of low levels of Nd as oxide. Chemical Geology, 94, 13–22.

Thirlwall M.F. and Anczkiewicz R. (2004)
Multidynamic isotope ratio analysis using MC-ICP-MS and the causes of secular drift in Hf, Nd and Pb isotope ratios. International Journal of Mass Spectrometry, 235, 59–81.

Wang Y.Q., Huang X.X., Sun Y.L., Zhao S.Q. and Yue Y.H. (2017)
A new method for the separation of LREEs in geological materials using a single TODGA resin column and its application to the determination of Nd isotope compositions by MC-ICP-MS. Analytical Methods, 9, 3531–3540.

references

Wasserburg G.J., Jacobsen S.B., DePaolo D.J., McCulloch M.T. and Wen T. (1981)
Precise determination of Sm/Nd ratios, Sm and Nd isotopic abundances in standard solutions. Geochimica et Cosmochimica Acta, 45, 2311–2323.

Waterton P., Pearson D.G., Kjarsgaard B., Hulbert L., Locock A., Parman S. and Davis B. (2017)
Age, origin and thermal evolution of the ultra-fresh ~ 1.9 Ga Winnipegosis Komatiites, Manitoba, Canada. Lithos, 268–271, 114–130.

Webb P.C., Thompson M., Potts P.J., Gowing C.J.B. and Meisel T.C. (2016)
Geo*PT*38A - an international proficiency test for analytical geochemistry laboratories – special report on round 38A (Modified harzburgite, HARZ01) / June 2016 (delayed). International Association of Geoanalysts. https://www.geoanalyst.org/wp-content/uploads/2017/10/GeoPT38AProvisionalReport.pdf

Weis D., Kieffer B., Maerschalk C., Barling J., Jong J.D., Williams G.A., Hanano D., Pretorius W., Mattielli N., Scoates J.S., Goolaerts A., Friedman R.M. and Mahoney J.B. (2006)
High-precision isotopic characterization of USGS reference materials by TIMS and MC-ICP-MS. Geochemistry, Geophysics, Geosystems, 7, Q08006.

Xiong Q., Griffin W.L., Zheng J.P., O'Reilly S.Y., Pearson N.J., Xu B. and Belousova E.A. (2016)
Southward trench migration at ~ 130–120 Ma caused accretion of the Neo-Tethyan forearc lithosphere in Tibetan ophiolites. Earth and Planetary Science Letters, 438, 57–65.

Xu Y.M., Wang G.Q., Yang Z., Zeng Y.L. and Guo F. (2024)
A single-column separation procedure for Sr, Nd and Sm in small-size samples and high-precision isotope measurements using a TIMS with 10^{13} and 10^{12} Ω amplifiers. Journal of Analytical Atomic Spectrometry, 39, 86–98.

Yang M., Yang Y.H., Kamo S.L., Romer R.L., Roberts N.M.W., Wang H., Xie L.W., Huang C., Yang J.H. and Wu F.Y. (2022)
Natural allanite reference materials for *in situ* U-Th-Pb and Sm-Nd isotopic measurements by LA-(MC)-ICP-MS. Geostandards and Geoanalytical Research, 46, 169–203.

Yang Y.H., Chu Z.Y., Wu F.Y., Xie L.W. and Yang J.H. (2011)
Precise and accurate determination of Sm, Nd concentrations and Nd isotopic compositions in geological samples by MC-ICP-MS. Journal of Analytical Atomic Spectrometry, 26, 1237–1244.

Yang Y.H., Wu F.Y., Li Q.L., Rojas-Agramonte Y., Yang J.H., Li Y., Ma Q., Xie L.W., Huang C., Fan H.R., Zhao Z.F. and Xu C. (2019)
In situ U-Th-Pb dating and Sr-Nd isotope analysis of bastnäsite by LA-(MC)-ICP-MS. Geostandards and Geoanalytical Research, 43, 543–565.

Yang Y.H., Wu F.Y., Wilde S.A., Liu X.M., Zhang Y.B., Xie L.W. and Yang J.H. (2009)
In situ perovskite Sr-Nd isotopic constraints on petrogenesis of the Mengyin kimberlites in the North China Craton. Chemical Geology, 264, 24–42.

Yang Y.H., Wu F.Y., Xie L.W. and Zhang Y.B. (2010a)
High-precision measurements of the ^{143}Nd/^{144}Nd isotope ratio in certified reference materials without Nd and Sm separation by multiple collector inductively coupled plasma-mass spectrometry. Analytical Letters, 43, 142–150.

Yang Y.H., Wu F.Y., Yang J.H., Chew D.M., Xie L.W., Chu Z.Y., Zhang Y.B. and Huang C. (2014)
Sr and Nd isotopic compositions of apatite reference materials used in U-Th-Pb geochronology. Chemical Geology, 385, 35–55.

Yang Y.H., Yang M., Jochum K.P., Wu S.T., Zhao H., Xie L.W., Huang C., Zhan X.C., Yang J.H. and Wu F.Y. (2020)
High-precision Sr-Nd-Hf-Pb isotopic composition of Chinese geological standard glasses CGSG-1, CGSG-2, CGSG-4 and CGSG-5 reference materials by MC-ICP-MS and TIMS. Geostandards and Geoanalytical Research, 44, 567–579.

Yang Y.H., Zhang H.F., Chu Z.Y., Xie L.W. and Wu F.Y. (2010b)
Combined chemical separation of Lu, Hf, Rb, Sr, Sm and Nd from a single rock digest and precise and accurate isotope determinations of Lu-Hf, Rb-Sr and Sm-Nd isotope systems using multi-collector ICP-MS and TIMS. International Journal of Mass Spectrometry, 290, 120–126.

Zhou T., Qi L., Liu S.H. and Zhou B. (2024)
A simplified instrumental protocol for trace Nd and Hf isotope measurements (< 10 ng) using a MC-ICP-MS and an Apex Omega de-solvating system. Journal of Analytical Atomic Spectrometry, 39, 2694–2702.